Coordination Chemistry Reviews 253 (2009) 2450–2459

Contents lists available at ScienceDirect

Coordination Chemistry Reviews

journal homepage: www.elsevier.com/locate/ccr

Review

Spin transition in octahedral metal complexes containing tetraazamacrocyclic ligands

Hans-Jörg Krüger*

Fachbereich Chemie, Technische Universität Kaiserslautern, Erwin-Schrödinger Straße 54, 67663 Kaiserslautern, Germany

Contents

ARTICLE INFO

Article history:
Received 23 March 2009
Accepted 12 June 2009
Available online 21 June 2009

Keywords:
Spin crossover
Tetraazamacrocycle
Iron(II) complexes
Iron(III) complexes
Cobalt(II) complexes
Cis-octahedral coordination environment
Trans-octahedral coordination environment

ABSTRACT

This review focusses on spin crossover complexes with octahedral metal ions which are bound to a tetraazamacrocyclic ligand and additionally either to two monodentate ligands or to one bidentate ligand. Macrocyclic ligands with a sufficiently large ring size prefer to coordinate to metal ions in an equatorial fashion yielding trans-octahedral coordination environments. In contrast, twelve-membered tetraazamacrocycles with high steric rigidity, such as 2,11-diaza[3.3](2,6)pyridinophanes or 2,11-dithia[3.3](2,6)pyridinophane, are prone to form cis-octahedral complexes. While the electronic and the steric properties of the coordinated tetraazamacrocycle in trans-octahedral complexes are very likely responsible for the paucity of observed spin transitions, the cis-octahedral coordination mode of the twelve-membered tetraazamacrocycles allows the preparation of an increasing number of mono- and oligonuclear spin crossover complexes with octahedral iron(II), iron(III) and cobalt(II) ions.

1. Introduction

Despite the tremendous insights that have been gained over the past decades into the underlying electronic principles responsible for the occurrence and the specific behavior of spin transition processes, the study of spin crossover complexes is still a highly attractive research field due to their potential application in developing electronic devices [1]. A comprehensive survey covering all aspects of spin crossover has recently been published in three volumes; it also serves as a valuable source of references leading to earlier reviews as well as to important original contributions in this area of research [2].

For the purpose of this account, only a few of the basic aspects of spin crossover will be discussed here. The spin crossover phenomenon is based on a temperature-, pressure- or light-induced change of the electronic state of a metal ion to one with a different spin multiplicity. For example, octahedral iron(II) spin crossover complexes possess a $^1A_{1g}$ ground state (low-spin state) arising from a $(t_{2g})^6$ electron configuration. If the excited $^5T_{2g}$ state (high-spin state) is sufficiently close in energy to the ground state ($\leq 200\,\text{cm}^{-1}$), it can be thermally populated by raising the temperature. In the excited state a $(t_{2g})^4(e_g)^2$ electron configuration is adopted. The occupation of σ-antibonding e_g-orbitals in the high-spin state results in a substantial elongation of the bonds between the iron(II) ion and the ligand donor atoms. Upon shifting from the low-spin (ls) state to the high-spin (hs) state, an increase of approximately 0.2 Å is generally observed in the iron-ligand bond lengths in iron(II) complexes.

---

* Fax: +49 631 2054676.
E-mail address: krueger@chemie.uni-kl.de.

0010-8545/$ – see front matter © 2009 Elsevier B.V. All rights reserved.
doi:10.1016/j.ccr.2009.06.004

This review concentrates on spin crossover complexes which contain a tetraazamacrocyclic coligand bound to an octahedral metal ion. Two types of tetraazamacrocyclic ligands can be identified on the basis of their modes of coordination to metal ions. If the macrocyclic ring encompasses thirteen or more atoms, the ligand prefers to bind to the metal ion in an equatorial fashion, leaving two *trans*-oriented coordination sites open to two additional monodentate ligands. In contrast, twelve-membered tetraazamacrocyclic rings cannot bind to an octahedral metal ion in a planar fashion, but instead fold upon coordination to afford two cis-oriented coordination sites, which are available for binding two monodentate or one bidentate ligand. These two different coordination modes, leading to trans- and cis-octahedral coordination geometries, respectively, are expected to impose different constraints on potential spin crossover processes. In addition to the σ-donor strengths and the π-acceptor capabilities of the tetraazamacrocyclic and the two trans-binding ligands, in trans-octahedral complexes the “macrocyclic hole” size plays a decisive role in determining the spin state of the metal ion. In order for the macrocycle to accommodate to the substantial changes in bond lengths during the spin transition process, sufficient flexibility of the macrocyclic hole, caused by ruffling of the ligand backbone, is required. This fact may explain why only very few trans-octahedral metal complexes which undergo spin transition have been reported. In contrast, in cis-octahedral metal complexes the hole size of the macrocycle is less important, as the ligand can adapt more freely to the needs of the coordinated metal ion. Instead structural distortions due to the small ring size of the macrocycle and the mutual influence of one donor atom on the binding properties of the other, which is communicated via the ligand backbone, are expected to play a more important role in spin transition processes of cis-octahedral complexes.

2. Trans-octahedral spin crossover complexes containing tetraazamacrocyclic ligands

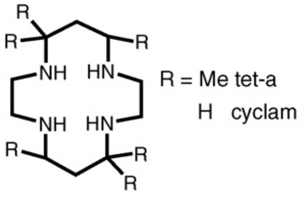

trans-[Fe(tet-a)(NCS)$_2$]

1

trans-[Fe(cyclam)Br$_2$](ClO$_4$)

2

There are very few recorded examples of octahedral spin crossover complexes which contain a tetraazamacrocyclic ligand bound to the metal ion in an equatorial fashion. In addition to the conditions mentioned above, the high in-plane ligand field strength of the equatorial macrocycle requires a combination of this ligand with sufficiently weak axial ligands for a spin transition to occur. Thus, an octahedral iron(II) complex **1**, containing thiocyanates in the axial positions and the hexamethyl derivative of the fourteen-membered tetraazamacrocyclic cyclam ligand (tet-a) in the equatorial plane, undergoes a gradual spin crossover when heated above room temperature [3]. With cyclam and two bromide ligands, spin crossover has been observed by EPR spectroscopy in the iron(III) complex **2** [4].

3. Cis-octahedral spin crossover complexes containing tetraazamacrocyclic ligands

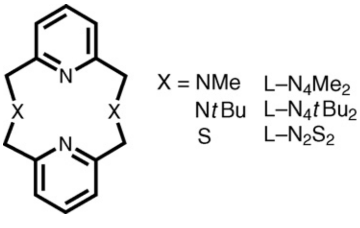

Derivatives of 2,11-diaza[3.3](2,6)pyridinophane (L-N$_4$R$_2$) and 2,11-dithia[3.3](2,6)pyridinophane (L-N$_2$S$_2$) are suitable ligands for enforcing a cis-octahedral coordination environment around metal ions [5]. Upon coordination, these ligands are folded along the N$_{\text{amine}}$–N$_{\text{amine}}$ or the S–S axis, respectively. Figs. 1–3 provide perspective views of the dithiocyanatoiron(II) complexes with these three ligands, demonstrating their coordination modes. The nitrogen atoms of the pyridine rings and the nitrogen donor atoms of the thiocyanato ligands form the equatorial coordination planes in these complexes, while the amine nitrogen atoms and the thioether sulfur atoms are bound to the metal ions at the axial coordination sites. The presence of the pyridine units endows the tetradentate ligand with a high degree of steric rigidity. This and the small macrocyclic ring size are responsible for the rather distorted octahedral coordination environment around the metal ion, as evidenced by the considerable deviation of the N$_{\text{amine}}$–Fe–N$_{\text{amine}}$ (144–162°) and the S–Fe–S angle (157–172°), respectively, from the ideal octahe-

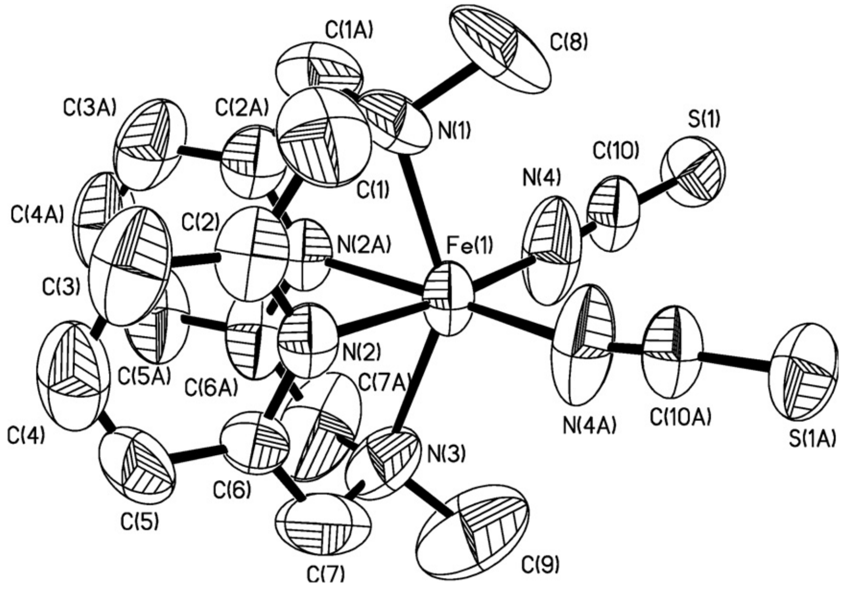

Fig. 1. Perspective view of the complex [Fe(L-N$_4$Me$_2$)(NCS)$_2$] (**3**).

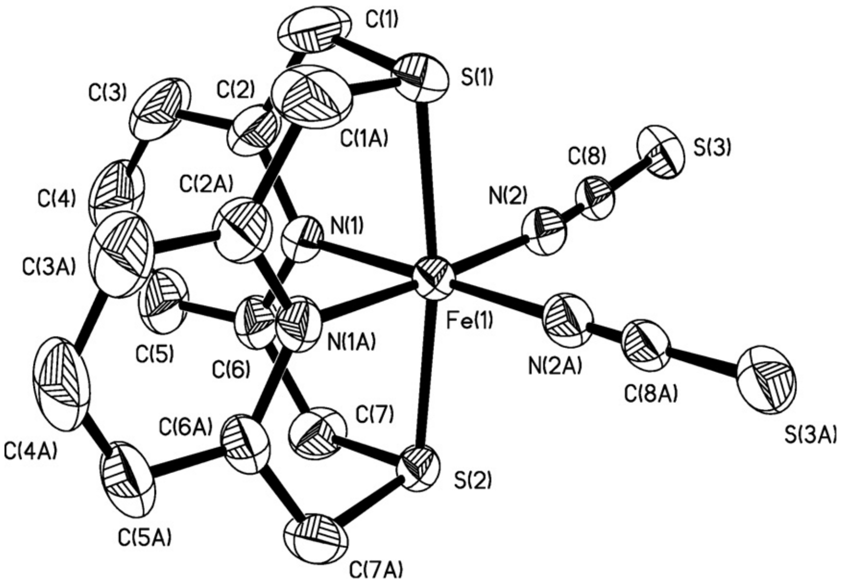

Fig. 2. Perspective view of the complex [Fe(L-N_2S_2)$(NCS)_2$] (**4**).

dral value of 180°. Past surveys of the metal–nitrogen bond lengths in octahedral metal complexes with these macrocycles, [5a,b] and the examples given in this overview (Tables 2, 4, 6–8), show that the equatorial M–N_{py} bonds are substantially shorter than the axial M–N_{amine} bonds. The amine substituents are located above and below the two thiocyanato ligands at the cis-oriented coordination sites. With the increasing size of the substituents, substantial steric interactions can be observed between the amine substituents and those ligands at the cis-oriented coordination sites. Thereby, the M–N_{amine} bonds are considerably increased in complexes containing L-$N_4t$$Bu_2$ as coligand. In addition, the ligand backbone is twisted, resulting in an approximate C_2 symmetry for the [M(L-$N_4t$$Bu_2$)] fragment as compared to the approximate C_{2v} symmetry of the [M(L-N_4Me_2)] fragment where little steric interaction occurs between the amine substituents and the cis-oriented ligands. The lengths of the M–N_{amine} and the M–N_{py} bonds are controlled by the filling of σ-antibonding e_g orbitals with electrons and can, therefore, be used as diagnostic tools in determining the spin state of the metal ion.

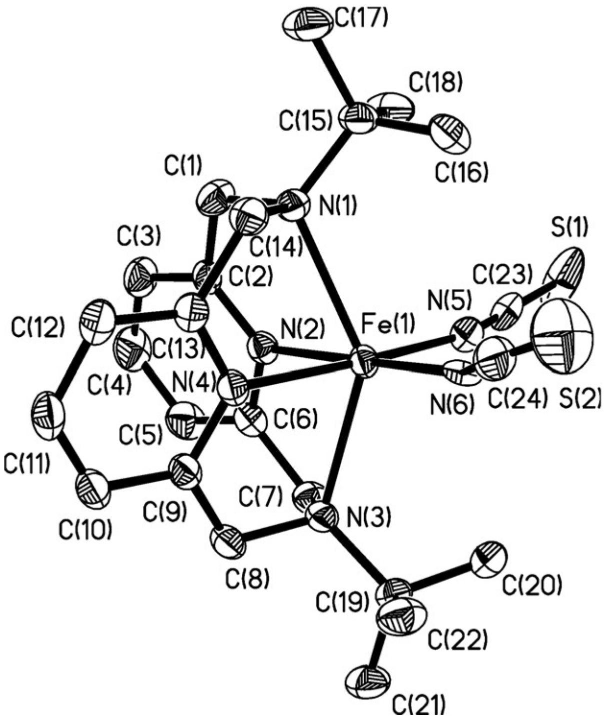

Fig. 3. Perspective view of the complex [Fe(L-$N_4t$$Bu_2$)$(NCS)_2$] (**5**).

3.1. Mononuclear iron(II) spin crossover complexes

[Fe(L–N_4Me_2)$(NCS)_2$]	[Fe(L–N_2S_2)$(NCS)_2$]·0.5 DMF	[Fe(L–$N_4t$$Bu_2$)$(NCS)_2$]
3	**4**	**5**

This discussion starts with a series of dithiocyanatoiron(II) complexes containing L-N_4Me_2, L-N_2S_2 or L-$N_4t$$Bu_2$ as coligands [6,7]. The structures of these complexes are displayed in Figs. 1–3. The investigation of the magnetic properties reveals that complexes **3** and **4** undergo spin transitions, while complex **5** remains in a hs ground state throughout the entire temperature range. The latter observation is related to the reduced ligand field strength of L-$N_4t$$Bu_2$ due to the elongated Fe–N bonds. For complex **3**, an abrupt spin transition at 236 K with a hysteresis of 6 K is observed (Fig. 4).

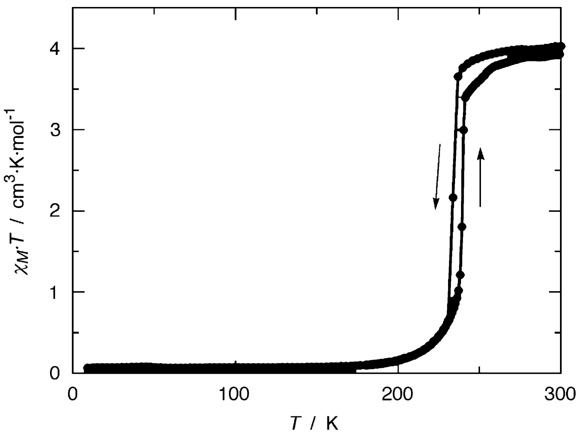

Fig. 4. Variation of the product $\chi_M \cdot T$ with temperature for solid **3** in a magnetic field of 0.5 T.

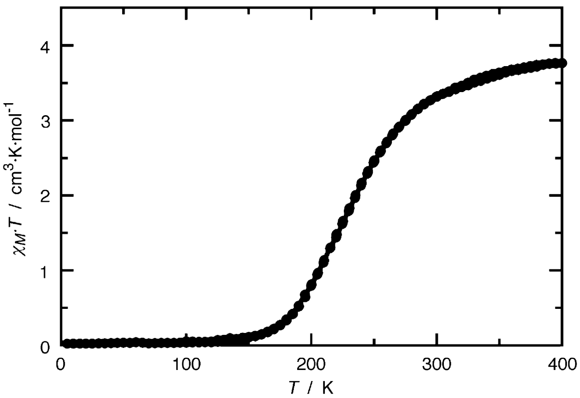

Fig. 5. Variation of the product $\chi_M \cdot T$ with temperature for solid **4** in a magnetic field of 0.2 T.

Table 1
Comparison of the spin crossover properties of the mononuclear iron(II) complexes.

Complex	Type of spin transition	Spin transition temperature (K)
3	Abrupt with hysteresis of 6 K	236
4	Gradual (140–400 K)	232
6	Gradual (120–180 K)	141
7	Gradual (220 to >400 K)[a]	≈320
9	Gradual (80–275 K)	177
10	Gradual (125–225 K)	179
11	Gradual (200 to >400 K)[a]	≈350
12	Gradual (200 to >400 K)[a]	≈335
13	Gradual (250 to >400 K)[a]	≈385

[a] Spin crossover was not completed at 400 K.

In contrast, the spin transition of complex **4**, occurring at almost the same spin transition temperature (232 K), is gradual, requiring a temperature range of 260 K for completion (Fig. 5). Additional spin crossover complexes **6**–**8** containing the tetraazamacrocycle L-N_4Me_2 as coligands could be obtained with the bidentate ligands gly^{1-}, pyc^{1-} and pyS^{1-} [6,8].

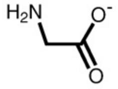
gly^{1-}

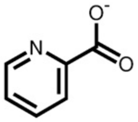
pyc^{1-}

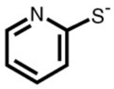
pyS^{1-}

[Fe(L–N_4Me_2)(gly)](ClO_4)·MeCN

6

[Fe(L–N_4Me_2)(pyc)](ClO_4)

7

[Fe(L–N_4Me_2)(pyS)](ClO_4)

8

The spin crossover properties were characterized by magnetic susceptibility measurements, X-ray structure analysis and Mössbauer spectroscopy. The corresponding data are collected in Tables 1–3. The bond lengths listed in Table 2 are compared to those of typical hs as well as ls complexes. As can be seen, in complex **3** the Fe–N_{py} and the Fe–N_{amine} bond lengths differ by 0.25 and 0.23 Å, respectively, between the ls and the hs complex and are characteristic for the respective spin state of the metal ion. The Mössbauer data in Table 3 agree with the magnetic susceptibility data of Table 1. In general, in iron(II) complexes with the ligands L-N_4Me_2 and L-N_2S_2, large quadrupole splittings of >1.65 mm s^{-1} at δ of 0.75–1.05 mm s^{-1} are detected for the hs complexes, and small quadrupole splittings of <0.50 mm s^{-1} at δ of 0.40–0.50 mm s^{-1} for the ls complexes.

Table 2
Comparison of selected bond lengths in iron(II) complexes containing the ligands L-N_4Me_2 or L-N_2S_2.

Complex	Temperature (K)	Fe–N_{py} (Å)	Fe–N_{amine} (Å)	Fe–X (Å)	
Low-spin complex					
[Fe(L-N_4Me_2)$(CN)_2$]		1.923	2.081		
Spin crossover complexes					
3	173	1.894	2.056	Fe–N	1.931
	293	2.143	2.282	Fe–N	2.038
6	133	1.974	2.138	Fe–N	2.048
				Fe–O	1.978
	293	2.131	2.275	Fe–N	2.160
				Fe–O	2.012
7	193	1.896	2.070	Fe–N	1.952
				Fe–O	1.968
	293	1.951	2.115	Fe–N	2.002
				Fe–O	1.966
8	150	1.896	2.082	Fe–N	1.957
				Fe–S	2.373
	373	2.127	2.269	Fe–N	2.134
				Fe–S	2.427
High-spin complex					
[Fe(L-N_4Me_2)Cl_2]		2.177	2.298		

Complex	Temperature (K)	Fe–N_{py} (Å)	Fe–S (Å)	Fe–N (Å)
4	173	1.977	2.250	1.948
	293	2.214	2.437	2.047

Table 3
Comparison of Mössbauer data in mononuclear and dinuclear iron(II) complexes containing the ligands L-N_4Me_2 or L-N_2S_2.

Complex	Temperature (K)	δ (mm s^{-1})	ΔE_Q (mm s^{-1})
Mononuclear complexes			
3	170	0.41	0.40
	310	0.97	2.10
4	110	0.42	0.14
	400	0.86	2.50
6	20	0.47	0.29
	293	0.95	2.16
7	100	0.42	0.35
	425	0.78	1.68
8	100	0.46	0.56
	293	0.80	2.84
Dinuclear complexes			
16	100	0.45 (53%)	0.30
		1.04 (47%)	3.72
	293	0.96 (100%)	3.32
17	100	0.47 (48%)	0.47
		1.02 (52%)	3.28
	293	0.91 (100%)	2.36

Table 4
Comparison of selected bond lengths in iron(II) complexes containing the ligand L-$N_4t Bu_2$.

Complex	Temperature (K)	Fe–N_{py} (Å)	Fe–N_{amine} (Å)	Fe–N_{cis} (Å)
Low-spin complex				
[Fe(L-$N_4t Bu_2$)$(CN)_2$]		1.914	2.172	
Spin crossover complexes				
9	113	1.932	2.232	1.967
	293	2.107	2.409	2.124
10	113	1.923	2.221	1.963
	293	2.114	2.397	2.140
11	113	1.908	2.196	1.994
	293[a]	1.922	2.224	2.006
12	150	1.901	2.191	1.982
	293[a]	1.955	2.261	2.036
13	150	1.911	2.199	1.964
	293[a]	1.920	2.216	1.967
High-spin complexes				
[Fe(L-$N_4t Bu_2$)Cl_2]		2.143	2.449	
5		2.137	2.403	

[a] Spin crossover was not completed at 293 K.

Table 5
Comparison of Mössbauer data in mononuclear iron(II) complexes containing the ligand L-$N_4t Bu_2$.

Complex	Temperature (K)	δ (mm s^{-1})	ΔE_Q (mm s^{-1})
Low-spin complex			
[Fe(L-$N_4t Bu_2$)$(CN)_2$]	110	0.32	2.14
Spin crossover complexes			
9	50	0.50	1.80
	293	0.88	1.49
10	50	0.50	1.67
	293	0.89	1.37
11	50	0.48	1.73
	293	0.47	1.63
	400	0.85	1.27
12	120	0.48	1.76
	400[a]	0.52	1.42
13	130	0.43	2.16
	400[a]	0.56	1.17
High-spin complexes			
[Fe(L-$N_4t Bu_2$)Cl_2]	293	1.02	2.82
5	293	1.00	2.61

[a] Spin transition is not completed at 400 K.

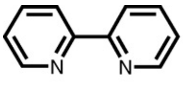

bipy

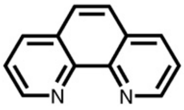

phen

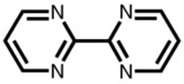

bpym

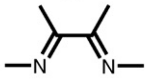

bmi

[Fe(L–$N_4t Bu_2$)(bipy)]$(BPh_4)_2$·MeCN·Et_2O

9

[Fe(L–$N_4t Bu_2$)(phen)]$(BPh_4)_2$·Et_2O

10

[Fe(L–$N_4t Bu_2$)(phen)]$(BPh_4)_2$·MeCN

11

[Fe(L–$N_4t Bu_2$)(bpym)]$(BPh_4)_2$·MeCN

12

[Fe(L–$N_4t Bu_2$)(bmi)]$(BPh_4)_2$

13

In order to obtain spin crossover complexes containing L-$N_4t Bu_2$ as coligand, the low ligand field strength of L-$N_4t Bu_2$ has to be counteracted by stronger ligands at the cis-oriented coordination sites. The right overall ligand field strength can be achieved with diimine ligands, such as bipy, phen, bpym or bmi [7,8]. Magnetic susceptibility measurements (Table 1) reveal more or less gradual spin transition processes for complexes **9**–**13**. Most of these complexes possess spin transition temperatures above room temperature. With phen as the additional ligand, the two crystalline substances **10** and **11**, which differ in the content of solvent molecules in the crystal lattice, could be isolated. These two substances show different spin crossover behavior, emphasizing the profound effect that solvent molecules in the lattice can exert on spin transition processes. While a gradual spin transition takes place at 179 K within a temperature range of 100 K in **10**, the spin process for complex **11** has a spin transition temperature of 347 K and is not completed at 400 K. The structural and the Mössbauer data listed in Tables 4 and 5 support the magnetic data. The bond lengths of some of the high-temperature measurements are consistent with the fact that, for these complexes, the spin process has not been completed at that temperature. The quadrupole splitting constants in the Mössbauer spectra of the ls complexes are unusually large due to the large distortion of the octahedral coordination environment around the iron(II) ion imposed by the macrocyclic ligand. In iron(II) complexes with L-$N_4t Bu_2$ as coligand, the spin states of the metal ions can, in general, still be clearly distinguished on the basis of their isomer shifts δ.

In summary, quite a variety of monodentate and bidentate ligands can be combined with diazapyridinophane ligands to produce octahedral iron(II) spin crossover complexes. Most of the complexes discussed display gradual spin crossover processes. Only complex **3** undergoes an abrupt spin transition with the occurrence of a small hysteresis. The reasons for the rather small cooperativity in the solids of **4**, **6**, **7** and **9**–**13** may be related to the presence of counter anions or of solvent molecules in the crystal lattice, which reduce the extent of elastic interactions between the iron(II) complexes [2]. This lower degree of interaction is judged to be responsible for the reduced levels of cooperativity. In contrast, there are no solvent molecules or counter ions in the crystal lattice of **3**. Additionally, in all crystal lattices, there are no obvious weak-interaction pathways, e.g. hydrophobic interactions or hydrogen-bonding networks, discernible between the spin crossover complex entities. Based on the cell parameters of **3**, there is also no evidence for a phase transition. However, the structure analysis of this complex at low temperatures is impeded by the occurrence of incommensurable modulations; these might be linked to the appearance of the small hysteresis.

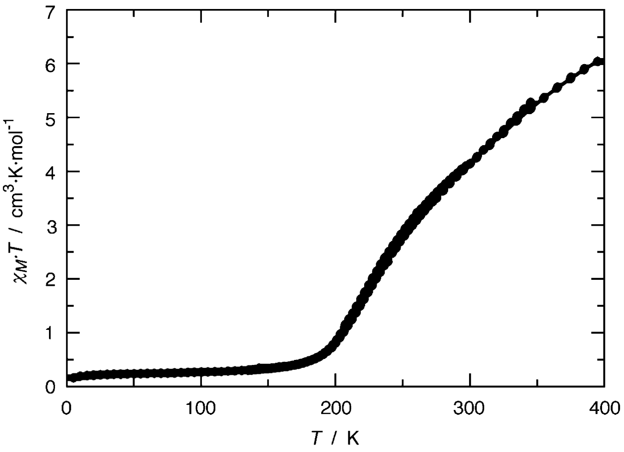

Fig. 6. Variation of the product $\chi_M \cdot T$ with temperature for solid **14** in a magnetic field of 0.5 T.

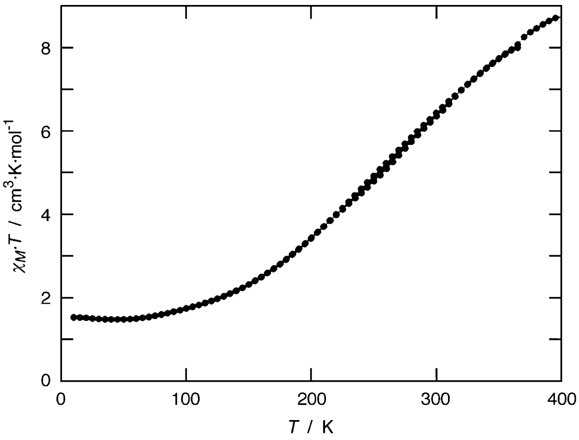

Fig. 7. Variation of the product $\chi_M \cdot T$ with temperature for solid **15** in a magnetic field of 0.5 T.

Nevertheless, at this point, the causes behind the occurrence of the hysteresis in **3** remain unresolved.

For the first time, to the best of my knowledge, spin crossover has been observed in cis-octahedral iron(II) complexes containing a tetraazamacrocyclic ligand. In addition to the generally observed $Fe^{II}N_6$ coordination sphere, spin transition has been established for complexes with $Fe^{II}N_4S_2$, $Fe^{II}N_5O$ and $Fe^{II}N_5S$ coordination environments. Further, some of the bidentate ligands can be easily modified so that further donor atoms can be incorporated into the ligand; these modified ligands allow the formation of multinuclear complexes without drastically disturbing the original electronic properties needed for spin transition at the iron site.

3.2. Di- and trinuclear iron(II) spin crossover complexes

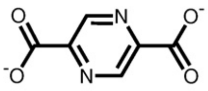

$pndc^{2-}$

$[\{Fe(L\text{–}N_4Me_2)\}_2(pndc)](ClO_4)_2\cdot H_2O$

14

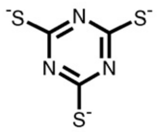

$ttcy^{3-}$

$[\{Fe(L\text{–}N_4Me_2)\}_3(ttcy)](ClO_4)_3\cdot 2H_2O$

15

Dinuclear and trinuclear spin crossover complexes were synthesized with the tetraazamacrocycle $L\text{-}N_4Me_2$ as coligand, using the potentially tetradentate or hexadentate ligands $pndc^{2-}$ and $ttcy^{3-}$ as bridging ligands [7,9]. In the resulting iron(II) complexes **14** and **15**, the individual iron sites are too widely separated from each other to allow any noteworthy electronic communication among them during spin transition. Thus, for complex **14** a gradual spin transition from a ls–ls to a hs–hs state is observed at temperatures above 200 K (Fig. 6). Currently it is not clear whether this spin transition occurs because of a direct conversion from a ls–ls to a hs–hs state or because of a two-step transition from a ls–ls via a ls–hs intermediate to a hs–hs state. There is a slight indication of a plateau occurring at 270 K which may be attributed to the existence of a ls–hs intermediate. However, further evidence, from structure analysis or a Mössbauer investigation in the presence of a magnetic field is needed to unambiguously support an interpretation of a two-step transition. A gradual, but at low temperatures incomplete spin transition from a ls–ls–ls to a hs–hs–hs state is observed for the trinuclear complex (Fig. 7). Here also, the question of whether the process is due a direct conversion or to a three-step transition is not resolved. The Mössbauer spectra at different temperatures corroborate the magnetic susceptibility data of **14** and **15**. Due to the poor quality of the crystals, no structural confirmation could be obtained for these complexes in order to support these observations.

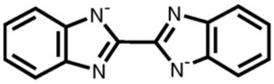

$bbzim^{2-}$

$[\{Fe(L\text{–}N_4Me_2)\}_2(bbzim)](ClO_4)_2\cdot 2EtCN$

16

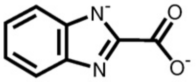

$bzimCO_2{}^{2-}$

$[\{Fe(L\text{–}N_4Me_2)\}_2(bzimCO_2)](ClO_4)_2\cdot 0.5(CH_3)_2CO$

17

In a study of a series of bipyrimidine-bridged dinuclear iron(II) complexes containing additionally mono- and bidentate ligands, microscopic two-step spin transitions between the three possible spin states (ls–ls, ls–hs and hs–hs states) were demonstrated [10]. For some bipyrimidine-bridged diiron(II) complexes, spin transition could only be enforced by the application of higher pressures; thus, depending on the applied pressure, the ls–hs or the ls–ls state could be achieved at low temperatures. In my research group we were hitherto unable to synthesize a similar bipyrimidine-bridged compound with the tetraazamacrocycle $L\text{-}N_4Me_2$. However, employing the dianionic ligands $bbzim^{2-}$ and $bzimCO_2{}^{2-}$ as bridging ligands, we were successful in synthesizing the dinuclear iron complexes **16** (Fig. 8) and **17**. Both complexes display spin transitions from a ls–hs ground state to a hs–hs state (Fig. 9, Table 3) at ambient pressure, with spin transition temperatures at 175 and 250 K for **16** and **17**, respectively. It is noteworthy that, in the crystal lattices of both complexes, there is a crystallographically distinct iron site which resides in the ls state at low temperatures (Table 6). A similar observation involving crystallographically distinct iron sites in a ls–hs dinuclear complex was made for complex **18** [11]. Here the two iron ions are separated by a diatomic bridge; this might be responsible for the strong electronic interaction between both iron ions and, thereby, for the occurrence of the ls–hs state.

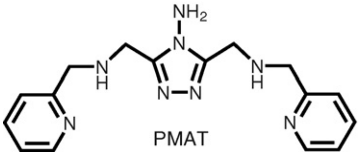

$[Fe_2(PMAT)_2](BF_4)_4\cdot DMF$

18

$[Fe(L\text{–}N_4Me_2)(bbzim)]\cdot 4MeOH$

19

$[Fe(L\text{–}N_4Me_2)(bpym)](ClO_4)_2$

20

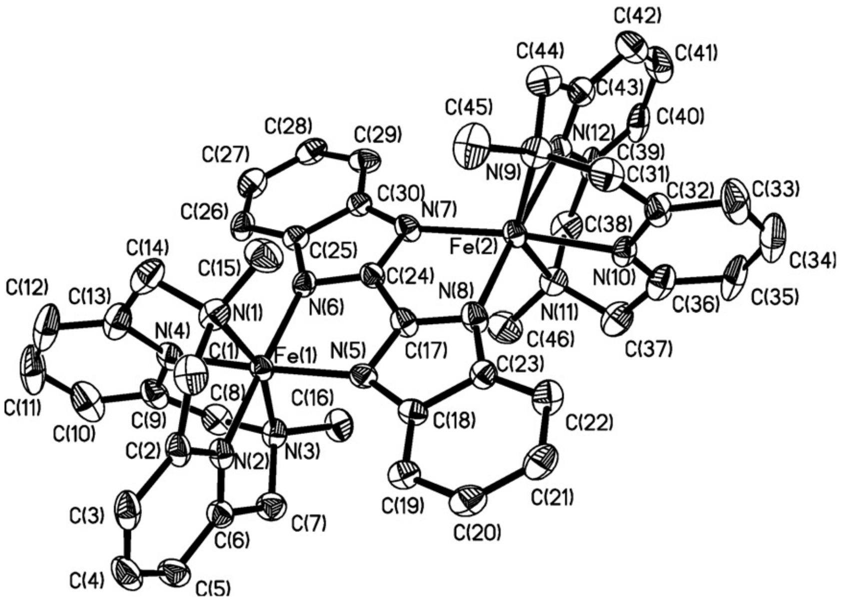

Fig. 8. Perspective view of the complex cation in **16** at 150 K.

We attribute the differences in spin crossover behavior between complex **16** and the previously reported bipyrimidine-bridged complexes to the presence of five-membered aromatic rings in the bridging moiety (Fig. 10). Due to the five-membered heterocyclic rings, the overlap between the filled orbitals of the nitrogen donor atoms and the metal ion orbitals is less optimal than in a bipyrimidine complex. This can be demonstrated by comparing the structures of the mononuclear ls iron(II) complexes **19** and **20**. In order to allow a better interaction with the ls iron(II) ion, the backbone of the bisbenzimidazolate ligand in **19** is considerably bent compared to that of the bipyrimidine ligand in **20**. Thus, the non-coordinating nitrogen atoms in the bisbenzimidazolate ligand of **19** are 3.15 Å apart, while the coordinated nitrogen atoms are separated by 2.57 Å. The difference in interatomic distances between the coordinated and the non-coordinating nitrogen atoms, respectively, are much less pronounced in **20** (2.61 and 2.78 Å). Thus, in the dinuclear complex **16** the interatomic N–N distance is 2.80 Å in the hs–hs complex, while in the ls–hs complex the interatomic distances are 2.71 and 2.90 Å, respectively, with the smaller distance observed between the nitrogen atoms which are coordinated to the ls iron ion. Due to the bending of the bridging ligand in **16**, the overlap between the bridging ligand and the hs iron ion is considerably reduced, thereby weakening the ligand field strength of the bridging unit on this side of the complex. The structural changes of the bridging ligand and the resulting variation of ligand field strength serve, in our opinion, as an explanation for our observation of a stable hs–ls ground state at ambient pressure. At least at ambient pressure, a ls–ls state cannot be achieved as the ground state for complex **16**. The question of whether a ls–ls state can be obtained upon application of higher pressures will be investigated in future studies.

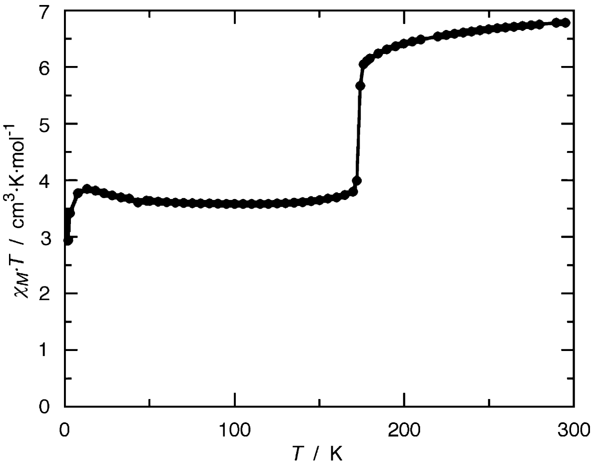

Fig. 9. Variation of the product $\chi_M \cdot T$ with temperature for solid **16** in a magnetic field of 0.5 T.

3.3. Cobalt(II) spin crossover complexes

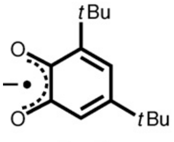

dbsq⁻

$[Co(L\text{–}N_4tBu_2)(dbsq)][B(C_6H_4Cl)_4]$

21

The spin crossover chemistry of octahedral cobalt(II) ions is generally restricted to strong-field ligands; [10c,12] this makes the observation that the cobalt(II) 3,5-di-*tert*butyl-semiquinonate complex **21** with L-N$_4t$Bu$_2$ as coligand undergoes a gradual spin crossover all the more surprising [13]. Magnetic susceptibility measurements (Fig. 11) reveal that a S = 1 spin state prevails at up to 200 K, arising from the ferromagnetic coupling of the S = 1/2 spin of the low-spin cobalt(II) ion with the S = 1/2 spin of the semiquinonate radical ligand. The increasing magnetic susceptibility at temperatures above 200 K is only consistent with the occurrence of a spin crossover. The structural data of **21**, as well as those of some typical hs and ls cobalt(II) complexes with this macrocyclic ligand, are compiled in Table 7. The structural data of **21** support the description of the electronic ground state as ls cobalt(II) semiquinonate on the basis of the long Co–N$_{amine}$ and the short Co–N$_{py}$ bond lengths. In addition, the averaged C–O bond length of 1.313 Å is consistent with the assignment of a semiquinonate redox state. The structure analysis of the complex at 400 K shows an increase of the Co–N$_{py}$ bond lengths, while the Co–N$_{amine}$ bonds essentially preserve their lengths. These results support the interpretation that a change of the $(t_{2g})^6(e_g)^1$ electron configuration in the ls state to a $(t_{2g})^5(e_g)^2$ electron configuration in the hs state

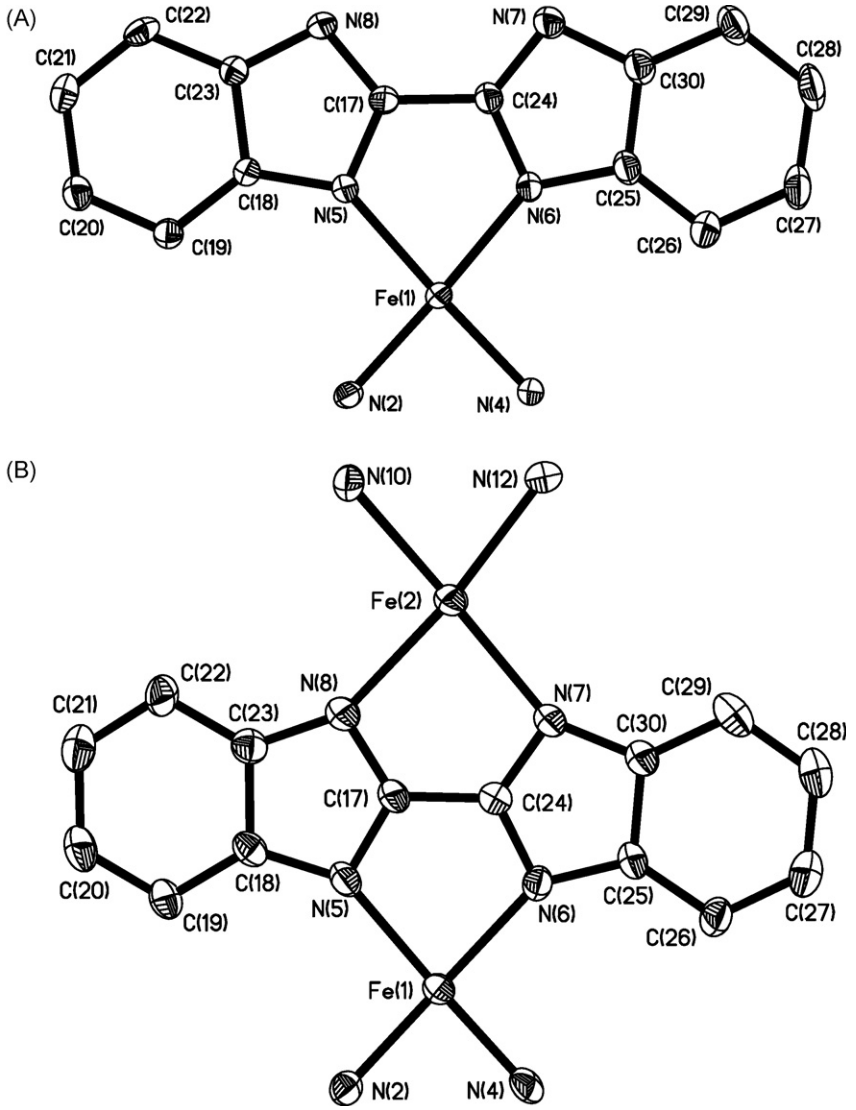

Fig. 10. View from the top onto the planes of the coordinated bisbenzimidazolate ligands in (A) **19**, and (B) ls–hs **16**, emphasizing the bending of the ligand backbone.

Table 6
Comparison of selected bond lengths in the dinuclear iron(II) complexes **16** and **17**.

Complex	Temperature (K)	Fe(1)–N_{py} (Å)	Fe(1)-N_{amine} (Å)	Fe(2)–N_{py} (Å)	Fe(2)–N_{amine} (Å)
16[a]	150	1.906	2.087	2.139	2.273
	293	2.125	2.250	2.125	2.250
17	150	1.893	2.071	2.148	2.262
	293	2.108	2.248	2.140	2.262

[a] At high temperatures, both halves of the hs–hs complex cation **16** are related by a crystallographic inversion centre, which is eliminated in the ls–hs state at low temperatures.

occurs. This observation is also interesting from a different point of view. Until now, any temperature-induced change of the spin state in cobalt dioxolene complexes has been linked to valence tautomerism, where a ls cobalt(III) catecholate complex is converted to a hs cobalt(II) semiquinonate complex with increasing temperatures [14]. Obviously the macrocyclic ligand L-$N_4t$$Bu_2$ still exerts enough ligand field strength to enforce the ls ground state, but it cannot supply enough electron density to the metal ion to stabilize the cobalt(III) oxidation state.

$[Co(L{-}N_4tBu_2)(NCS)_2]$ $[Co(L{-}N_4Me_2)(NCS)_2]$

22 **23**

If a temperature-induced spin transition is possible for complex **21**, then it should also be feasible to find other non-redoxactive ligands, which would allow a spin transition to occur, for the two cis-oriented coordination sites. The right conditions were met in the dithiocyanatocobalt(II) complex **22**, where a comparison of the bond lengths at 110 and 293 K (Table 7) clearly demonstrates a spin transition, which is still incomplete at 110 K. Interestingly, the corresponding dithiocyanatocobalt(II) complex **23** with L-N_4Me_2 contains a hs cobalt(II) ion even at low temperatures. In contrast to the analogous iron(II) complexes **3** and **5**, the influence of the ligand field strength on the existence of a temperature-induced spin transition in a complex seems to be reversed in complexes **22** and **23**. It

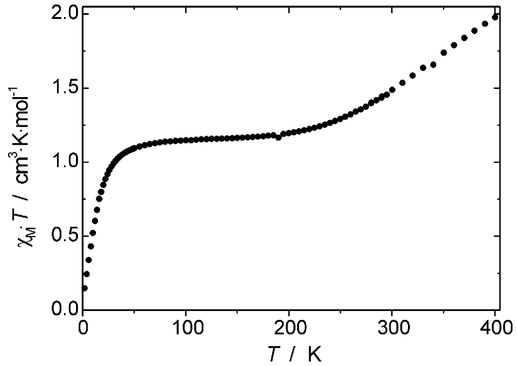

Fig. 11. Variation of the product $\chi_M \cdot T$ with temperature for solid **21** in a magnetic field of 0.5 T.

Table 7
Comparison of selected bond lengths in mononuclear cobalt(II) complexes containing the ligand L-N_4tBu_2.

Complex	Temperature (K)	Co–N_{py} (Å)	Co–N_{amine} (Å)[a]	Co–X_{cis} (Å)
Low-spin complex				
[Co(L-N_4tBu_2)(ampy)]$^{2+}$[b]		1.910	2.387 2.400	
Spin crossover complexes				
21	100	1.931	2.308 2.368	1.890
	400[c]	1.991	2.320 2.371	1.969
22	110[d]	2.007	2.332 2.379	1.984
	293	2.072	2.345 2.413	2.034
High-spin complex				
[Co(L-N_4tBu_2)Cl_2][e]		2.089	2.351 2.460	

[a] There is a substantial deviation in length between the two Co–N_{amine} bonds; therefore each bond length is listed, in contrast to the Co–N_{py} bond lengths, which are very similar to each other.
[b] ampy = 2-aminomethylpyridine.
[c] Spin crossover was not completed at 400 K.
[d] Spin crossover was not completed at 110 K.
[e] Data taken from reference [5b].

should, however, be kept in mind, that the spin transition temperature is not only controlled by enthalpic factors, but, according to the equation $T_c = \Delta H/\Delta S$, also by entropic contributions. Therefore, we attribute the observation of the spin transition in **22**, despite the lower ligand field strength of L-N_4tBu_2, to a rather small entropic change during spin transition.

3.4. Iron(III) spin crossover complexes

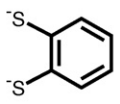

$S_2C_6H_4^{2-}$

[Fe(L–N_4Me_2)($S_2C_6H_4$)](ClO_4)·0.5H_2O
24

A highly unusual temperature-induced spin transition with $T_c \approx 170$ K from a ls S = 1/2 ground state to an intermediate S = 3/2 spin state has been observed in the octahedral iron(III) benzenedithiolate complex **24**, containing the macrocycle L-N_4Me_2 [15]. The assignment of the excited state as an intermediate iron(III) state is based on structural (Table 8), ESR, magnetic and Mössbauer data. Thus, the Fe–N_{amine} bonds become substantially elongated upon raising the temperature, while the Fe–N_{py} bonds remain approximately the same. Taking into account that the Fe–N bond lengths are quite characteristic for the spin state of the metal ion, the observed bond lengths at higher temperatures are consistent with a $(d_{xy}, d_{xz}, d_{yz})^4(d_{z^2})^1(d_{x^2-y^2})^0$ electron configuration. The detection of a S = 3/2 signal in the ESR-spectrum supports this interpretation. A possible alternate interpretation, in which at high temperature a hs iron(II) dithiosemiquinonate state is obtained due to valence tautomerism, is not supported by the structural data. The observation of an excited intermediate spin state has been attributed to the rather distorted octahedral coordination environment and to the strong covalent bonds between the benzenedithiolate ligand and the iron(III) ion in the equatorial plane.

Table 8
Comparison of selected bond lengths in mononuclear iron(III) complexes containing the ligand L-N_4Me_2.

Complex	Temperature (K)	Fe–N_{py} (Å)	Fe–N_{amine} (Å)
Low-spin complex			
[Fe(L-N_4Me_2)(bipy)]$^{3+}$		1.902	2.044
Spin crossover complex			
24	153	1.979	2.144
	293	2.020	2.222
High-spin complexes			
[Fe(L-N_4Me_2)Cl_2]$^+$		2.130	2.232
[Fe(L-N_4Me_2)(cat)]$^{+}$[a]		2.106	2.223

[a] cat^{2-} = catecholate.

4. Conclusions

Employing twelve-membered macrocyclic ligands L-N_4R_2 as coligands allows a modular approach in obtaining new spin crossover complexes with a large variety of ligands. This allows a systematic study of the electronic properties in spin crossover complexes containing a common structural motif. In addition, the resulting distortion of the octahedral coordination environment around the metal ion due to the structural and steric properties of the macrocycle can lead to unexpected results in the field of spin crossover chemistry.

Acknowledgements

I gratefully acknowledge the financial support from the Deutsche Forschungsgemeinschaft within the Priority Program “Molecular Magnetism” (SPP 1137), from the Technische Universität Kaiserslautern and from the research centre OPTIMAS. In addition, I would like to express my gratitude to my present and past coworkers Dr. M. Graf, Dr. W. Koch, Dr. H. Kelm, S. Reh and M. Vetter as well as to Franc Meyer’s research group at the University of Göttingen for their good collaborations.

References

[1] (a) O. Kahn, J.P. Launey, Chemtronics 3 (1988) 140;
(b) J.-F. Letard, P. Guionneau, L. Goux-Capes, Top. Curr. Chem. 235 (2004) 221.
[2] P. Gütlich, H.A. Goodwin (Eds.), Spin Crossover in Transition Metal Compounds I–III, Springer, Berlin, 2004 (Top. Curr. Chem. 233–235 (2004)).
[3] J.C. Dabrowiak, P.H. Merrel, D.H. Busch, Inorg. Chem. 11 (1972) 1979.
[4] A. Desideri, J.B. Raynor, J. Chem. Soc., Dalton Trans. (1977) 2051.
[5] (a) H.-J. Krüger, Chem. Ber. 128 (1995) 531;
(b) S.P. Meneghetti, P.J. Lutz, J. Fischer, J. Kress, Polyhedron 20 (2001) 2705;
(c) E.C. Constable, J. Lewis, V.E. Marquez, P.R. Raithby, J. Chem. Soc., Dalton Trans. (1986) 1747.
[6] (a) M. Graf, H. Kelm, G. Wolmershäuser, S. Demeschko, F. Meyer, H.-J. Krüger, unpublished results;
(b) M. Graf, Diplomarbeit, TU Kaiserslautern, 2003.
[7] (a) M. Graf, H. Kelm, G. Wolmershäuser, S. Demeschko, F. Meyer, H.-J. Krüger, unpublished results;
(b) M. Graf, Dissertation, TU Kaiserslautern, 2009.

[8] (a) S. Reh, H. Kelm, G. Wolmershäuser, S. Demeschko, F. Meyer, H.-J. Krüger, unpublished results;
(b) S. Reh, Diplomarbeit, TU Kaiserslautern, 2007.
[9] (a) M. Vetter, H. Kelm, G. Wolmershäuser, S. Demeschko, F. Meyer, H.-J. Krüger, unpublished results;
(b) M. Vetter, Diplomarbeit, TU Kaiserslautern, 2006.
[10] (a) J.A. Real, A.B. Gaspar, M.C. Munoz, P. Gütlich, V. Ksenofontov, H. Spiering, Top. Curr. Chem. 233 (2004) 167;
(b) A.B. Gaspar, M.C. Munoz, J.A. Real, J. Mater. Chem. 16 (2006) 2522;
(c) K.S. Murray, Eur. J. Inorg. Chem. (2009) 3101.
[11] M.H. Klingele, B. Moubaraki, J.D. Cashion, K.S. Murray, S. Brooker, Chem. Commun. (2005) 987.
[12] (a) I. Krivokapic, M. Zerara, M. Lawson Daku, A. Vargas, C. Enachescu, C. Ambrus, P. Tregenna-Piggott, N. Amstutz, E. Krausz, A. Hauser, Coord. Chem. Rev. 251 (2007) 364;
(b) U. Beckmann, S. Brooker, Coord. Chem. Rev. 245 (2003) 17;
(c) H.A. Goodwin, Top. Curr. Chem. 234 (2004) 23;
(d) J. Zarembowitch, New J. Chem. 16 (1992) 255.
[13] M. Graf, G. Wolmershäuser, H. Kelm, S. Demeschko, F. Meyer, H.-J. Krüger, submitted for publication.
[14] (a) D.A. Shultz, in: J.S. Miller, M. Drillon (Eds.), Magnetism: Molecules to Materials, vol. II, Wiley-VCH, Weinheim, 2001, p. 281;
(b) D.N. Hendrickson, C.G. Pierpont, Top. Curr. Chem. 234 (2004) 63;
(c) C.G. Pierpont, Coord. Chem. Rev. 216–217 (2001) 99;
(d) Beni, C. Carbonera, A. Dei, J.-F. Létard, R. Righini, C. Sangregorio, L. Sorace, J. Braz. Chem. Soc. 17 (2006) 1522.
[15] W.O. Koch, V. Schünemann, M. Gerdan, A.X. Trautwein, H.-J. Krüger, Chem. Eur. J. 4 (1998) 686.